Optimal Reciprocal Collision Avoidance for Multiple Non-Holonomic Robots

Javier Alonso-Mora, Andreas Breitenmoser, Martin Rufli, Paul Beardsley and Roland Siegwart

Abstract In this paper an optimal method for distributed collision avoidance among multiple non-holonomic robots is presented in theory and experiments. Non-holonomic optimal reciprocal collision avoidance (NH-ORCA) builds on the concepts introduced in [2], but further guarantees smooth and collision-free motions under non-holonomic constraints. Optimal control inputs and constraints in velocity space are formally derived for the non-holonomic robots. The theoretical results are validated in several collision avoidance experiments with up to fourteen e-puck robots set on collision course. Even in scenarios with very crowded situations, NH-ORCA showed to be collision-free for all times.

1 Introduction

Multi-robot systems are designed to achieve tasks by collaboration. A key requirement for their efficient operation is good coordination and reciprocal collision avoidance. Moving a vehicle on a collision-free path is a well-studied problem in robot navigation. The work in [4], [6] and [8] presents representative examples of collision avoidance methods for single mobile robots. Basically, similar approaches as in the single robot cases can be applied in the context of collision avoidance for multiple robots. However, the increase in robot density and collaborative interaction needs methods that scale well with the number of robots. The collision avoidance approaches are extended in [11] among others for multiple robots by decoupling path planning and coordination. Other work investigated potential fields [5] and cooper-

Javier Alonso-Mora, Andreas Breitenmoser, Martin Rufli and Roland Siegwart
Autonomous Systems Laboratory (ASL), ETH Zurich, Tannenstrasse 3, 8092 Zurich, Switzerland
e-mail: {jalonso, andrbrei, ruflim, rsiegwart}@ethz.ch

Javier Alonso-Mora, Paul Beardsley
Disney Research Zurich, Clausiusstrasse 49, 8092 Zurich, Switzerland
e-mail: {jalonso, pab}@disneyresearch.com

ative control laws [14] to direct a group of robots to their objectives while avoiding collisions. Decentralized control helps lowering computational cost and introduces additional robustness and flexibility to the multi-robot system.

In this paper, we develop and formally analyze a new collision avoidance strategy for a group of non-holonomic robots. Mobile robots we see being deployed nowadays in research or industry are mostly non-holonomic. Therefore installations with multiple robots in real world scenarios, such as multiple vacuum cleaners or collaborative monitoring and maintenance vehicles, require collision avoidance methods that take the non-holonomic constraints of the robots into account.

Our approach builds on Optimal Reciprocal Collision Avoidance (ORCA) [2] and extends it toward *non-holonomic* reciprocal collision avoidance. The robots are controlled to stay within a maximum tracking error $\mathscr{E}$ of an ideal holonomic trajectory. Control inputs for optimal tracking are derived from mapping holonomic onto non-holonomic velocities. We focus on differential-drive robots in the following work, even though our approach applies more generally for the class of feedback-linearizable vehicles with non-holonomic kinematics, such as car-like robots or differentially-driven robots with trailer.

Reciprocal Collision Avoidance (RVO) [3], a collaborative collision avoidance method based on velocity obstacles, was reformulated as ORCA [2] and shown to be solved efficiently through a low-dimensional linear program, which results in completeness and a speed-up of the algorithm. Each robot makes a similar collision avoidance reasoning and collision-free motion is guaranteed all time, but holonomic robots are assumed and oscillations in the form of reciprocal dances can occur. The extension in [12] combines both the concepts of basic velocity obstacles and RVO to reduce the amount of oscillations. In addition, robot kinematics and sensor uncertainty are included by enlarging the velocity cones, even though a formal proof of collision-free motion is not given. The work in [15] generalizes RVO for robots with non-holonomic constraints by testing sampled controls for their optimality. As the method requires extensive numeric computation and relies on probabilistic sampling, it may fail to find an existing feasible solution. The latest extension [13] introduces a solution for differential-drive robots by applying ORCA on the robot's virtual center. This is in contrast to our approach of extending the robot's radius, which allows to decrease its extension to zero in crowded scenarios. [13] also relies on the mapping between desired holonomic and non-holonomic velocities, but is different from ours in how it is derived; moreover it further constrains the motion of the robots. Another reactive collision avoidance method for unicycles based on velocity obstacles was presented in [9], where inputs are obtained by a weighted combination of the closest collision in normal and tangential directions.

The paper is organized as follows. We start with the problem formulation in Section 2 and review the main concepts of ORCA. Then the proposed algorithm for collision avoidance in a group of non-holonomic robots is presented in Section 3. In Section 4, we give a formal analysis of the non-holonomic controls that lead to optimal tracking of holonomic velocities and prove collision-free motion. Section 5 demonstrates the method in experiments with up to fourteen robots and shows successful collision avoidance and smooth trajectories.

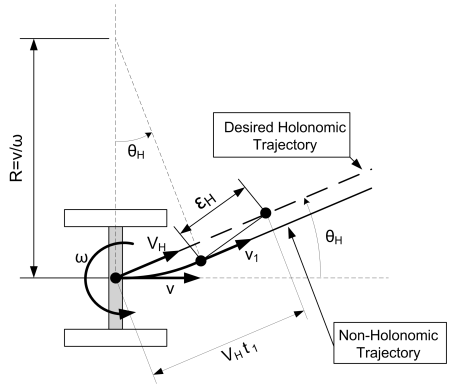

Fig. 1 Non-holonomic tracking error. The holonomic trajectory is tracked by the differential-drive robot moving along the non-holonomic trajectory within tracking error ε_H.

2 Problem formulation

2.1 Kinematic model of differential-drive robot

First the kinematic model for the differential-drive robot is introduced. The basic trajectories of the non-holonomic robots considered in this work are defined by two sections, an arc of circumference covered with constant speed v, followed by a straight line path with constant speed v_1, as illustrated in Fig. 1. The basic non-holonomic controls $(v(t), \omega(t))$ consist of the linear and angular velocities

$$v(t) = \begin{cases} v = \omega R, \text{ for } 0 \le t \le t_1 \\ v_1, \text{ for } t > t_1 \end{cases}, \qquad \omega(t) = \begin{cases} \omega, \text{ for } 0 \le t \le t_1 \\ 0, \text{ for } t > t_1 \end{cases}. \tag{1}$$

Note that in our formulation the robots have no constraints in acceleration, nevertheless, these could be easily included by adding to the complexity of the formulation. Although the planned trajectory is a circular sector followed by a straight line segment, the robots perform only a part of the circular segment and then recompute, which results in final trajectories that are much more complex.

The kinematic constraints are given by $|v(t)| \le v_{max,\omega} = v_{max} - |\omega(t)|\frac{l_w}{2}$, $|\omega(t)| \le \omega_{max} = \frac{2v_s^{max}}{l_w K_{vs}}$ and $v_{max} = \frac{v_s^{max}}{K_{vs}}$, where the wheel speed is bounded by $-v_s^{max} \le v_s(t) = \left(v(t) \pm \frac{l_w}{2}\omega(t)\right) K_{vs} \le v_s^{max}$, with $v_s(t)$ the angular velocity of the right and the left wheel respectively, l_w is the distance between the wheels and K_{vs} a conversion factor. The system parameters that are relevant for the locomotion of the e-puck robot (refer to Section 5) are given by: $l_w = 0.0525$ m, $v_s^{max} = 1000$ steps/s, $K_{vs} = 7674.6$ steps/m, $v_{max} = 0.13$ m/s and $\omega_{max} = 4.96$ rad/s.

The *set of non-holonomic controls* $S_{NHC} = \{(v(t), \omega(t)) \,|\, \text{Eq. (1) and kinematic constraints}\}$ is defined as the feasible subset of the controls $(v(t), \omega(t))$ given by Eq. (1), i.e. the controls satisfying the kinematic constraints.

2.2 Set of allowed holonomic velocities

The underlying idea of the approach here presented is that a particular non-holonomic robot is able to track a certain set of holonomic motions within a given maximum tracking error $\mathscr{E}$. Therefore, increasing the radius of each robot by its fixed value $\mathscr{E}$ guarantees collision-free trajectories, even in the case of non-holonomic robots. The tracking error ε_H is quantified by consideration of the robot's kinematics and can be bounded by a certain value $\mathscr{E}$ through limiting the set of holonomic trajectories to be tracked.

In Fig. 1 the trajectories for both holonomic and non-holonomic robots are presented. If the velocity v_1 of the non-holonomic robot in Eq. (1) is fixed to the speed of the holonomic robot V_H, the maximum error in tracking a holonomic trajectory at constant velocity $\mathbf{v}_H = V_H(\cos(\theta_H), \sin(\theta_H))$ is given at time t_1, and represented by ε_H. Note that the tracking error might as well be decreased with a more complex control scheme. However, it never increases under the non-holonomic controls according to Eq. (1). Let us fix $v_1 = V_H$ in the following.

Thus, for a given holonomic velocity $\mathbf{v}_{H_i} = \mathbf{v}_H$ and control inputs (v, ω) at time $t = k\Delta t$, where $k \in \mathbb{N}$ is the iteration index and Δt the time step, the value of the tracking error ε_H is given by simple geometry

$$\begin{aligned} \varepsilon_H^2(v, w, V_H, \theta_H) &= (V_H t_1 - R\sin(\theta_H))^2 + (R(1-\cos(\theta_H)))^2 \\ &= V_H^2 t_1^2 - \frac{2V_H t_1 \sin(\theta_H)}{\omega} v + \frac{2(1-\cos(\theta_H))}{\omega^2} v^2. \end{aligned} \tag{2}$$

For non-holonomic robots and fixed a maximum tracking error $\mathscr{E}$, the *set of allowed holonomic velocities* S_{AHV} is given by the velocities $\mathbf{v}_H$ for which there exists a control input within the set of non-holonomic controls S_{NHC} that guarantees a tracking error lower or equal than the given maximum tracking error $\mathscr{E}$ at all times. The set of allowed holonomic velocities is defined as

$$S_{AHV} = \{\mathbf{v}_H \in \mathbb{R}^2 \mid \exists (v(\tau), \omega(\tau)) \in S_{NHC},\ ||\mathbf{p} + \tau \cdot \mathbf{v}_H - \hat{\mathbf{p}}^k(\tau)|| \leq \mathscr{E}\ \forall \tau \geq 0\}, \tag{3}$$

where $\hat{\mathbf{p}}^k(\tau)$ is the expected robot position at time $k\Delta t + \tau$ if controls $(v(\tau), \omega(\tau))$ are applied at time $k\Delta t$.

In order to obtain smooth trajectories, the time t_1 to achieve the correct orientation θ_H can be fixed to a minimum value T. Note that this value must be at least equal to the time step Δt of the controller. t_1 is kept fixed for the following sections.

In Section 4 the closed form of S_{AHV} and the mapping between the sets S_{AHV} and S_{NHC}, as well as the proof of collision-free motion, are derived.

2.3 Optimal reciprocal collision avoidance

ORCA [2] is a velocity-based approach to collision avoidance that provides a sufficient condition for guaranteeing collision-free motion among multiple holonomic robots. Given a group of n disk-shaped robots with radius r_i and velocity $\mathbf{v}_i \in \mathbb{R}^2$ at position $\mathbf{p}_i$ in the plane $\mathbb{R}^2$, each robot tries to reach an assigned goal point $\mathbf{g}_i$ by selecting a preferred velocity $\mathbf{v}_i^{pref} \in \mathbb{R}^2$. The objective is to choose an optimal $\mathbf{v}_i$, which lies as close as possible to $\mathbf{v}_i^{pref}$, such that collisions among the robots are avoided for at least a time horizon τ.

In the case of holonomic robots with velocities $\mathbf{v}_H \in \mathbb{R}^2$, the velocity obstacle for robot $i \in [1,n] \subset \mathbb{N}$ with r_i at $\mathbf{p}_i$ induced by any robot $j \in [1,n]$, $j \neq i$, with r_j at $\mathbf{p}_j$ is defined as the set of relative velocities $\bar{\mathbf{v}} = \mathbf{v}_{H_i} - \mathbf{v}_{H_j}$ between robots i and j

$$VO_{i|j}^{\tau} = \left\{ \bar{\mathbf{v}} \,|\, \exists t \in [0,\tau], t \cdot \bar{\mathbf{v}} \in D(\mathbf{p}_j - \mathbf{p}_i, r_i + r_j) \right\}, \tag{4}$$

with $D(\mathbf{p},r) = \{\mathbf{q} \,|\, \|\mathbf{q}-\mathbf{p}\| < r\}$ the open ball of radius r. The set of collision-free velocities $ORCA_{i|j}^{\tau}$ for robot i with respect to robot j can geometrically be constructed from $VO_{i|j}^{\tau}$ (see Fig. 2 left and center). First, the minimum change

$$\mathbf{u} = (\underset{\bar{\mathbf{v}} \in \partial VO_{i|j}^{\tau}}{argmin} \|\bar{\mathbf{v}} - (\mathbf{v}_i^{opt} - \mathbf{v}_j^{opt})\|) - (\mathbf{v}_i^{opt} - \mathbf{v}_j^{opt}), \tag{5}$$

which needs to be added to $\bar{\mathbf{v}}$ to avoid a collision, is computed. $\mathbf{v}_i^{opt}$ is the optimization velocity, set to the current velocity $\mathbf{v}_{H_i}^{current}$ of the robot. This gives good results as shown in [2]. Then $ORCA_{i|j}^{\tau} = \{\mathbf{v}_{H_i} | (\mathbf{v}_{H_i} - (\mathbf{v}_i^{opt} + c\mathbf{u})) \cdot \mathbf{n} \geq 0\}$ follows as described in [2]. $\mathbf{n}$ denotes the outward normal of the boundary of $VO_{i|j}^{\tau}$ at $(\mathbf{v}_i^{opt} - \mathbf{v}_j^{opt}) + \mathbf{u}$, and c defines how much each robot gets involved in avoiding a collision. $c = \frac{1}{2}$ means both robots i and j help to equal amounts to avoid colliding with each other; $c = 1$ means robot i fully avoids collisions with a dynamic obstacle j. Likewise, the velocity obstacle can be computed for static obstacles following [2].

The set of collision-free velocities for robot i, $ORCA_i^{\tau}$, is given by

$$ORCA_i^{\tau} = S_{AHV_i} \cap \bigcap_{j \neq i} ORCA_{i|j}^{\tau}, \tag{6}$$

with S_{AHV_i} the set of allowed holonomic velocities under the kinematic constraints of robot i. For holonomic robots, $S_{AHV_i} = D(0, V_{H_i}^{max})$. Fig. 2 on the right shows the set $ORCA_i^{\tau}$ for a configuration with multiple robots, where S_{AHV_i} is approximated by the convex polygon P_{AHV_i} for a differential-drive robot.

The optimal holonomic velocity for robot i is to be found as

$$\mathbf{v}_{H_i}^{*} = \underset{\mathbf{v}_{H_i} \in ORCA_i^{\tau}}{argmin} \|\mathbf{v}_{H_i} - \mathbf{v}_i^{pref}\|. \tag{7}$$

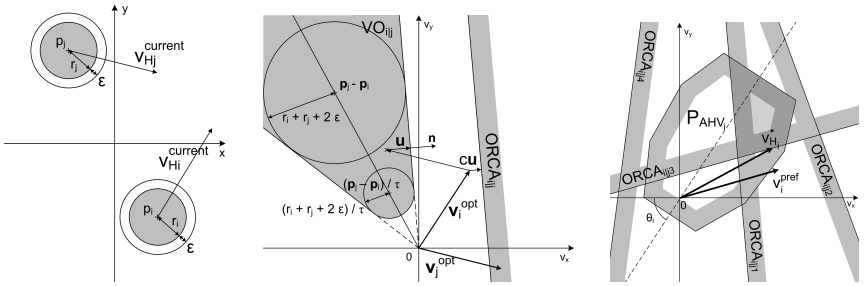

Fig. 2 Left: configuration with two non-holonomic robots. Center: $VO^{\tau}_{i|j}$ and $ORCA^{\tau}_{i|j}$ for a holonomic robot at $\mathbf{p}_i$ with $r_i+\varepsilon$ and $\mathbf{v}_{H_i}^{current}$, generated by a holonomic robot at $\mathbf{p}_j$ with $r_j+\varepsilon$ and $\mathbf{v}_{H_j}^{current}$. Right: constraints in velocity generated by $ORCA^{\tau}_{i|j}$ from multiple robots, together with the set P_{AHV_i} taking into account the kinematics of the robot. The region of collision-free velocities $ORCA^{\tau}_i$ is highlighted and $\mathbf{v}^*_{H_i}$ is displayed.

3 NH-ORCA: Optimal reciprocal collision avoidance under non-holonomic constraints

In each time-step NH-ORCA consists of the following three main steps: first, $VO^{\tau}_{i|j}$ and $ORCA^{\tau}_{i|j}$ are computed for holonomic robots of radius $r_i+\mathscr{E}_i$, $r_j+\mathscr{E}_j$ at $\mathbf{p}_i$, $\mathbf{p}_j$ with velocity $\mathbf{v}_{H_i}^{current}$, $\mathbf{v}_{H_j}^{current}$. Second, S_{AHV_i} is computed for fixed $\mathscr{E}_i$ and T_i and approximated by a convex polygon P_{AHV_i}. Moreover, $ORCA^{\tau}_i$ is generated with respect to the neighboring robots and an optimal holonomic velocity is selected from the set of collision-free velocities defined by Eq. (6); thereby, the preferred velocities of the robots are taken into account. This is represented in Fig. 2 where $\mathscr{E}=\mathscr{E}_i=\mathscr{E}_j$. Finally, the selected holonomic velocity is mapped to the corresponding non-holonomic control inputs, which guarantee collision-free motion. A detailed description of the algorithm is provided in Algorithm 1.

The closed-form expression from Eq. (13) (in Section 4) is evaluated to compute the maximum allowed holonomic velocities, this is the set S_{AHV_i}. In general, S_{AHV_i} is not convex for a given T_i. In our implementation of NH-ORCA, the area of S_{AHV_i} is approximated by a convex polygon P_{AHV_i} that lies inside S_{AHV_i}. This simplifies the optimization problem. Note that P_{AHV_i} can be precomputed due to rotational invariance and at each iteration be aligned with the current orientation of the robot. As $ORCA^{\tau}_i$ is a convex region formed by linear constraints, a quadratic optimization problem with linear constraints is formulated. Eq. (7), where S_{AHV_i} is substituted by P_{AHV_i}, can efficiently be solved by methods from computational geometry. The optimization velocity $\mathbf{v}_i^{opt}$ that is used in the optimization is set to the current holonomic velocity $\mathbf{v}_{H_i}^{current}$ of the agent, but other choices are possible. The mapping to non-holonomic optimal control inputs follows from Eq. (9) (in Section 4).

NH-ORCA can be applied to heterogeneous groups of robots with different kinematic constraints, sizes, maximum tracking errors $\mathscr{E}_i$ and lower bounds T_i.

Algorithm 1 Non-Holonomic Reciprocal Collision Avoidance.

Require: Fixed $\mathscr{E}_i$ and T_i. Group of differential-drive robots $i \in [1,n]$ provided with:
- internal parameters: $\mathbf{p}_i$, $\mathbf{v}_{H_i}^{current}$, θ_i, $\mathbf{v}_i^{pref}$, r_i, $\mathscr{E}_i$, T_i.
- external parameters (obtained from sensing or communication): $\mathbf{p}_j$, $\mathbf{v}_{H_j}^{current}$, $r_j + \mathscr{E}_j$ with $j \neq i$.

Compute $P_{AHV_{i,0}}$ from closed-form expression of $S_{AHV_{i,0}}$ and zero orientation, Eq. (13).
loop
  for $i \in \{1,...,n\}$ **do**
    Compute P_{AHV_i} by rotating $P_{AHV_{i,0}}$ to match orientation θ_i.
    for $j \in \{1,...,n\}$, $j \neq i$ **do**
      Compute $VO^{\tau}_{i|j}$ for holonomic robots of radius $r_i + \mathscr{E}_i$ and $r_j + \mathscr{E}_j$ at p_i and p_j with $\mathbf{v}_{H_i}^{current}$ and $\mathbf{v}_{H_j}^{current}$.
      Compute $ORCA^{\tau}_{i|j}$.
    end for
    Construct $ORCA^{\tau}_i = P_{AHV_i} \cap \bigcap_{i \neq j} ORCA^{\tau}_{i|j}$.
    Compute optimal collision-free holonomic velocity $\mathbf{v}^*_{H_i}$ following Eq. (7).
    Map $\mathbf{v}^*_{H_i}$ to (v_i, ω_i) following Eq. (9).
    Apply controls.
  end for
end loop

4 Formal analysis

In our analysis the symmetry of the tracking with respect to both axis and its rotational invariance is exploited. Therefore, the considerations are limited to the case of tracking holonomic velocities in $\mathbb{R}^2_+$ and zero orientation of the agent. It is clear that the analysis extends likewise to entire $\mathbb{R}^2$ and general orientation of the robot.

4.1 Selection of non-holonomic controls

In this section, the control inputs (v, ω) for optimal tracking of a given holonomic velocity $\mathbf{v}_H$ are found. The controls for the non-holonomic robot are chosen as those that minimize the tracking error ε_H, while achieving the correct orientation in the fixed given time T. If this is impossible due to the robot's constraints, the robot performs a turn in place by rotating at maximum speed until the correct orientation is reached, i.e. $\omega = \min\left(\frac{\theta_H}{T}, \omega_{max}\right)$. In general, t_1, θ_H and ω are related by $\omega = \frac{\theta_H}{t_1}$.

With everything else fixed, the linear velocity that minimizes Eq. (2) is given by

$$v^* = \frac{V_H t_1 \sin(\theta_H)\omega}{2(1-\cos(\theta_H))} = V_H \frac{\theta_H \sin(\theta_H)}{2(1-\cos(\theta_H))}. \tag{8}$$

The optimal linear velocity might not be feasible due to the limits on the linear and angular velocities. Therefore, the optimal controls are

$$\begin{aligned} R_{A1}: \ \omega &= \frac{\theta_H}{T} \leq \omega_{max} \ \text{ and } \ v = v^* \leq v_{max,\omega} \\ R_{A2}: \ \omega &= \frac{\theta_H}{T} \leq \omega_{max} \ \text{ and } \ v = v_{max,\omega} \\ R_B: \ \omega &= \omega_{max} \ \text{ and } \ v = 0. \end{aligned} \tag{9}$$

If the optimal controls are chosen, the maximum tracking error $\varepsilon_H^2(\mathbf{v}_H)$ committed in each of the regions are derived from Eq. (2) and Eq. (8) and given by

$$R_{A1}: \ \varepsilon_H^2 = \left(\frac{2(1-\cos(\theta_H)) - \sin^2(\theta_H)}{2(1-cos(\theta_H)} \right) T^2 V_H^2 \tag{10}$$

$$R_{A2}: \ \varepsilon_H^2 = V_H^2 T^2 - \frac{2V_H T^2 \sin(\theta_H)}{\theta_H} v_{max,\omega} + \frac{2T^2(1-\cos(\theta_H))}{\theta_H^2} v_{max,\omega}^2 \tag{11}$$

$$R_B: \ \varepsilon_H = V_H t_1 = V_H \frac{\theta_H}{\omega_{max}}. \tag{12}$$

4.2 Construction of S_{AHV}

The closed form of the set of allowed holonomic velocities S_{AHV} is derived for fixed $\mathscr{E}$ and T in this section. For a given orientation θ_H of the holonomic velocity, the maximum holonomic speed V_H that can be successfully tracked with $\varepsilon_H \leq \mathscr{E}$ is computed (see Fig. 3). Note that for feasibility, the maximum holonomic speed is limited by the robot's maximum linear velocity $V_H \leq v_{max}$. Otherwise the tracking error would increase after time t_1.

Theorem 1. *Both the optimal linear velocity $v(V_H)$ and the tracking error $\varepsilon_H(V_H)$ are monotonically increasing with respect to the holonomic speed V_H for fixed θ_H.*

Proof. From Eq. (8)-(9) it directly follows that, with everything else fixed, the optimal linear velocity v is monotonically increasing with respect to the holonomic speed V_H. The monotonicity of $\varepsilon_H(V_H)$ is derived from Eq. (10)-(12). Due to limited space, the proof is omitted. □

Theorem 2. *The maximum holonomic speed V_H^{max} that can be tracked with $\varepsilon_H \leq \mathscr{E}$ for a fixed θ_H is given by*

$$V_H^{max} = \begin{cases} \min\left(\frac{\mathscr{E}}{T} \sqrt{\frac{2(1-\cos(\theta_H))}{2(1-\cos(\theta_H))-\sin^2(\theta_H)}}, v_{max} \right) & \text{if} \quad \begin{cases} \frac{\theta_H}{T} \leq \omega_{max} \\ v_{\mathscr{E}}^* \leq v_{max,\omega} \end{cases} \\ \min\left(\frac{-\beta+\sqrt{\beta^2-4\alpha\gamma}}{2\gamma}, v_{max} \right) & \text{if} \quad \begin{cases} \frac{\theta_H}{T} \leq \omega_{max} \\ v_{\mathscr{E}}^* \geq v_{max,\omega} \end{cases} \\ \min\left(\frac{\mathscr{E}\omega_{max}}{\theta_H}, v_{max} \right) & \text{if} \quad \frac{\theta_H}{T} \geq \omega_{max}, \end{cases} \tag{13}$$

where $v^*_{\mathscr{E}}$, α, β, γ *are given by*

$$v^*_{\mathscr{E}} = \frac{\mathscr{E}}{T}\frac{\theta_H \sin(\theta_H)}{2(1-\cos(\theta_H))}\sqrt{\frac{2(1-\cos(\theta_H))}{2(1-\cos(\theta_H))-\sin^2(\theta_H)}}, \tag{14}$$

$$\alpha = T^2\,, \quad \beta = -\frac{2T^2\sin(\theta_H)}{\theta_H}v_{max,\omega}\,, \quad \gamma = \frac{2T^2(1-\cos(\theta_H))}{\theta_H^2}v^2_{max,\omega} - \mathscr{E}^2. \tag{15}$$

Proof. Denote $v_{\mathbf{v}_H^{max}}$ and $\omega_{\mathbf{v}_H^{max}}$ the linear and angular velocities for optimal tracking of the maximum holonomic velocity $\mathbf{v}_H^{max}$, given by V_H^{max} and θ_H.

The proof is divided for regions R_{A1}, R_{A2} and R_B. Recall from Theorem 1 that, $v(V_H)$ and $\varepsilon_H(V_H)$ are monotonically increasing with respect to V_H. This is implicitly used in the proof. In all cases the value of the maximum holonomic speed V_H^{max} must be limited to v_{max} following $V_H \leq v_{max}$.

- Region R_{A1}: Assume $\omega_{\mathbf{v}_H^{max}} = \frac{\theta_H}{T} < \omega_{max}$. Consider the case where $v_{\mathbf{v}_H^{max}} < v_{max,\omega}$. The holonomic speed which gives a tracking error equal to the maximum $\varepsilon_H = \mathscr{E}$ is found by solving Eq. (10), which gives the top value V_H^{max} of Eq. (13). The linear velocity for optimal tracking of $\mathbf{v}_H^{max}$ is then given by Eq. (14), obtained by substituting V_H^{max} into Eq. (8), which is feasible if $v^*_{\mathscr{E}} \leq v_{max,\omega} = v_{max} - \frac{\theta_H l_W}{2T}$. If this holds, $v_{\mathbf{v}_H^{max}} = v^*_{\mathscr{E}}$. Otherwise, the solution is found in region R_{A2}.

- Region R_{A2}: Assume $\omega_{\mathbf{v}_H^{max}} = \frac{\theta_H}{T} < \omega_{max}$. Consider the case where $v_{\mathbf{v}_H^{max}} = v_{max,\omega}$. The tracking error is given by Eq. (11) and from Theorem 1, the maximum holonomic speed V_H^{max} satisfies $\varepsilon_H = \mathscr{E}$. The solution is given by solving, $0 = \alpha(V_H^{max})^2 + \beta V_H^{max} + \gamma$, where from Eq. (11), $\alpha = T^2$, $\beta = -\frac{2T^2\sin(\theta_H)}{\theta_H}v_{max,\omega}$ and $\gamma = \frac{2T^2(1-\cos(\theta_H))}{\theta_H^2}v^2_{max,\omega} - \mathscr{E}^2$. From Theorem 1, the maximum holonomic speed is given by the solution of largest value, hence the middle value V_H^{max} of Eq. (13). The associated linear velocity for optimal tracking is given by $v_{\mathbf{v}_H^{max}} = v_{max,\omega} = v_{max} - \frac{\theta_H l_W}{2T}$. Finally, the value of the maximum holonomic speed V_H^{max} must be limited to v_{max} following $V_H \leq v_{max}$.

- Region R_B: Assume $\omega_{\mathbf{v}_H^{max}} = \omega_{max}$. In this case, a rotation in place is performed. Therefore $v_{\mathbf{v}_H^{max}} = 0$. Recalling Eq. (12) and Theorem 1, the maximum holonomic speed V_H^{max} from Eq. (13) bottom is obtained. □

Similar results are derived for the case where the angular velocity ω is limited by $\hat{\omega} < \omega_{max}$. This leads to smoother trajectories and, independently of the chosen T, in place rotations are avoided.

Theorem 3. *Consider $\omega \leq \hat{\omega} < \omega_{max}$. The maximum holonomic speed V_H^{max} that can be tracked with $\varepsilon_H \leq \mathscr{E}$ for a fixed θ_H is given by*

$$V_H^{max} = \begin{cases} \min\left(\frac{\mathscr{E}}{T} \sqrt{\frac{2(1-\cos(\theta_H))}{2(1-\cos(\theta_H))-\sin^2(\theta_H)}}, v_{max} \right) & \text{if} \quad \begin{cases} \frac{\theta_H}{T} \leq \hat{\omega} \\ v^*_{\mathscr{E}} \leq v_{max,\omega} \end{cases} \\ \min\left(\frac{-\beta+\sqrt{\beta^2-4\alpha\gamma}}{2\gamma}, v_{max} \right) & \text{if} \quad \begin{cases} \frac{\theta_H}{T} \leq \hat{\omega} \\ v^*_{\mathscr{E}} \geq v_{max,\omega} \end{cases} \\ \min\left(\frac{\mathscr{E}\hat{\omega}}{\theta_H} \sqrt{\frac{2(1-\cos(\theta_H))}{2(1-\cos(\theta_H))-\sin^2(\theta_H)}}, v_{max} \right) & \text{if} \quad \begin{cases} \frac{\theta_H}{T} \geq \hat{\omega} \\ v^*_{\mathscr{E}} \leq v_{max,\omega} \end{cases} \\ \min\left(\frac{-\hat{\beta}+\sqrt{\hat{\beta}^2-4\hat{\alpha}\hat{\gamma}}}{2\hat{\gamma}}, v_{max} \right) & \text{if} \quad \begin{cases} \frac{\theta_H}{T} \geq \hat{\omega} \\ v^*_{\mathscr{E}} \geq v_{max,\omega} \end{cases} \end{cases} \tag{16}$$

where $v^*_{\mathscr{E}}$, α, β, γ are given by Eq. (14) and (15). $\hat{\alpha}$, $\hat{\beta}$, $\hat{\gamma}$ are given by

$$\hat{\alpha} = \frac{\theta_H^2}{\hat{\omega}^2}, \quad \hat{\beta} = -\frac{2\theta_H \sin(\theta_H)}{\hat{\omega}^2} v_{max,\omega}, \quad \hat{\gamma} = \frac{2(1-\cos(\theta_H))}{\hat{\omega}^2} v_{max,\omega}^2 - \mathscr{E}^2. \tag{17}$$

Proof. The proof is analogous to that of Theorem 2, where the optimal controls are given by $\omega = \min(\frac{\theta_H}{T}, \hat{\omega})$ and $v = \min(v^*, v_{max,\omega})$. □

Remark 1 *Maximal S_{AHV}.* The maximal set of allowed holonomic velocities S_{AHV}^{max} is given by a maximization of the maximal holonomic speed V_H^{max} over T for a fixed orientation θ_H, $S_{AHV}^{max} = \bigcup_{T \in [\Delta t, \infty)} S_{AHV}$. In this case the time T is not constant, but varies as a function of the orientation θ_H.

Remark 2 *Polygonal approximation P_{AHV}.* Due to the particular non-convex shape of the S_{AHV} two options are described. First, the best approximation is obtained by dividing S_{AHV} in two complementary regions, one for forward and one for backward driving. Then, the problem is solved for one region (the one pointing towards the desired goal) and if unfeasible, for the opposite region in a second step. This region is represented by $P_{AHV,A}$ in Fig. 3. Alternatively, a faster but more restrictive implementation is obtained by using the biggest rectangle contained inside S_{AHV}. This region is represented by $P_{AHV,B}$ in Fig. 3 on the right.

Remark 3 *Behavior in the limits.* Two limit cases might be considered:

- Limit $T \to 0$. For $\theta_H = 0$ trajectories are straight lines; in fact, $\omega = 0$ holds independent of T and therefore perfect tracking is achieved for $V_H \leq v_{max}$. For $\theta_H \in (0, \frac{\pi}{2}]$ and fixed θ_H, $\frac{\theta_H}{T} \to \infty$ is obtained; therefore, rotation in place with $\omega = \omega_{max}$ and $v = 0$ is always the chosen trajectory. This reduces to time optimal trajectories, each composed of straight line segments alternating with turns in place as seen in [1].
- Limit $\mathscr{E} \to 0$. For $\theta_H = 0$ trajectories are straight lines; again, $\omega = 0$ holds independent of T and therefore perfect tracking is achieved for $V_H \leq v_{max}$. For $\theta_H \in (0, \frac{\pi}{2}]$, it can be seen from Theorem 2 that trajectories are reduced to turning in place at angular velocity $\omega = \min\left(\frac{\theta_H}{T}, \omega_{max}\right)$ and $v = 0$.

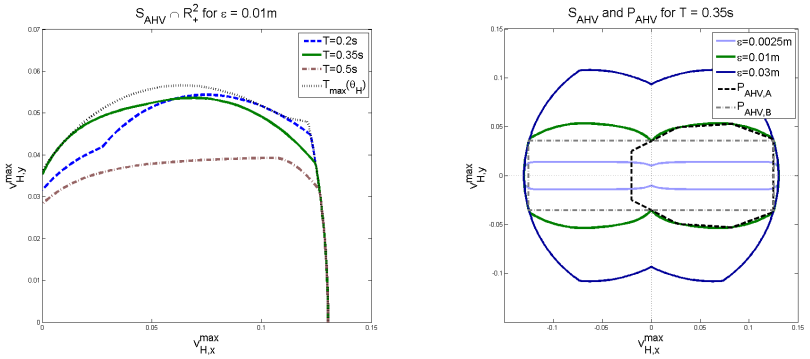

Fig. 3 Left: S_{AHV} for fixed $\mathscr{E}$ and varying T. $T_{max}(\theta_H)$ denotes the variable T that results in the maximal set S^{max}_{AHV}. Right: S_{AHV} for fixed T and varying $\mathscr{E}$. Two polygonal approximations $P_{AHV,A}$ and $P_{AHV,B}$ are shown for $\mathscr{E} = 0.01$ m and $T = 0.35$ s.

Remark 4 *Variable maximum tracking error $\mathscr{E}$.* NH-ORCA guarantees collision-free trajectories for non-holonomic robots, that is $r_i + r_j \leq d(\mathbf{p}_i, \mathbf{p}_j)$. To guarantee feasibility of the computation of the $VO^{\tau}_{i|j}$, $r_i + r_j + \mathscr{E}_i + \mathscr{E}_j \leq d(\mathbf{p}_i, \mathbf{p}_j)$ must be satisfied, i.e. the extended radii of the robots must not be in collision. This might happen for fixed $\mathscr{E}_i$ and $\omega_i \neq 0$ but is assuredly avoided by having $\mathscr{E}_i$ and $\mathscr{E}_j$ stepwise decreasing when robots are close to each other.

4.3 Collision-free motion

Finally, the proof that NH-ORCA guarantees collision-free motions among multiple non-holonomic robots is presented.

Theorem 4. *The trajectories of all robots are guaranteed to be collision-free.*

Proof. First, planned trajectories for the holonomic robots of radius $r_i + \mathscr{E}_i$ are collision-free, if solutions of ORCA exist, as proven in [2]. Otherwise the constraints given by $ORCA^{\tau}_{i|j}$ must be relaxed by decreasing τ until the problem becomes feasible, thus becoming a 3D optimization [2]. Second, planned trajectories for non-holonomic robots stay within distance $\mathscr{E}_i$ of the planned trajectories for extended holonomic robots, if $T_i \geq \Delta t$. Note that this only guarantees that the distance between two non-holonomic agents is greater than the sum of their radii. To guarantee feasibility of the velocity obstacles computation, and thus completion of the method, Remark 4 must hold in addition.

Trajectories planned for the non-holonomic robot are collision-free. Due to the time-discrete implementation, after each time-step a new collision-free trajectory is computed. Therefore, the trajectories of all agents, given as concatenation of segments, are collision-free. □

Remark 5 *Deadlocks.* NH-ORCA guarantees collision-free trajectories for non-holonomic robots but convergence to a goal destination is not fully guaranteed. While robots are in movement, deadlocks will not appear (as seen in our experiments in Section 5. Nevertheless, when robots reach their goal, their behavior is close to that of static obstacles. If they are approached by another robot, a deadlock situation may result as the robot's velocity that is closest to its preferred velocity might become zero in order to avoid collisions. This is inherited from the original method for holonomic agents [2] and can be resolved by waypoint navigation [7].

5 Experimental results

We have evaluated the proposed collision avoidance method and the theoretical results by experiments with real robots. A group of fourteen e-puck robots [10] is used in the experiments. The e-puck is a small disk-shaped differential-drive robot. To enable reliable communication and tracking of the e-pucks, the robots were enhanced with a generic radio receiver and eight infrared LEDs. Red-colored disks were further added on top of each robot for better visual appearance. The following parameters for the NH-ORCA computation are selected: $\mathscr{E} = 0.01$ m, $T = 0.35$ s, $\tau = 7$ s, $V^{pref} = 0.1$ m/s and $r = 0.05$ m the radius of the modified e-puck.

The test setup consists of a central workstation with radio transmitter and an overhead camera mounted on a frame above a flat floor plate of 1.2 m x 1.4 m. The robots' positions and orientations are detected and read into the workstation, where the NH-ORCA is computed for each robot in a decentralized way. The resulting velocities are then broadcasted to the e-pucks in each iteration. The e-puck robots and the workstation form a closed control loop running at a frequency of 10 Hz.

The results of two experiments are presented, which confirm the theoretical findings from Section 4. In the first experiment four e-puck robots are placed in square shape and consecutively exchange positions with each other. Fig. 4 on the left illustrates a subsequence of the robots exchanging positions in diagonal directions. On the right, the trajectories for two out of the four robots are shown when moving along the square's vertical edge to swap positions. As can be seen from the trajectories of the first experiment, not only collision-free but also smooth and visually appealing motions are obtained for the differential-drive robots with the NH-ORCA algorithm.

In cases of symmetry and in order to avoid reciprocal dances [12], the closest point on the velocity obstacle $VO^{\tau}_{i|j}$ is selected clockwise for Eq. (5). This gives preference to right-side avoidance in cases of full symmetry.

In the second experiment, fourteen e-pucks are lined up on a circle and move all together to their antipodal positions on the circle's boundary. This experiment demonstrates that the distributed NH-ORCA algorithm scales with the number of robots, and that it can moreover be applied without any change in the set of parameters for scenarios with many robots (the same parameters as in the first experiment with only four robots are used). The robots successfully solve a very crowded sce-

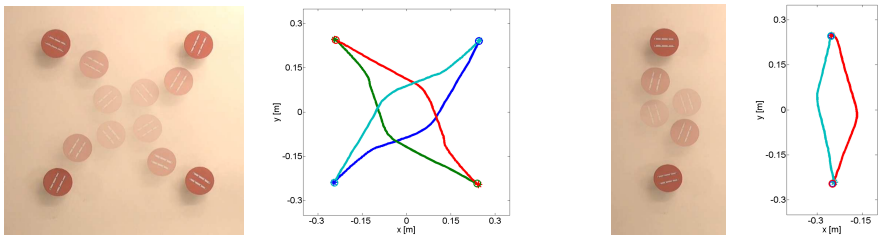

Fig. 4 Experiment 1 with four e-puck robots. Left: e-pucks exchanging positions in diagonal direction. Right: e-pucks exchanging positions vertically. Both sequences and trajectories are smooth and collision-free.

Fig. 5 Experiment 2 with fourteen e-puck robots. The sequence shows collision-free transition of the e-pucks through the circle center to the antipodal position on the circle's boundary.

nario while avoiding collisions at all times. In such scenarios with many robots, a slow-down of the robots can be noticed in areas of increased robot density. This results from the stronger constraints on the feasible set of velocities, and is in correspondence with Theorem 2 and Remarks 3 and 4 (tendency of increasingly turning in place).

In cases where the optimization becomes unfeasible, zero inputs can be selected for the robots. Alternatively, implementation of Remark 4 and of the 3D optimization guarantee feasibility while leading to a decrease in the time of collision τ. As a result, faster motions are achieved for the robots in Experiment 2. The robots can get infinitely close from the fact that no safety area is added, but collisions are avoided. Further experiments studied different scenarios, including scenarios with dynamic obstacles. A video showing the conducted experiments in full length accompanies the paper.

6 Conclusion and outlook

In this work, a fast and distributed method for local collision avoidance among non-holonomic robots, so-called NH-ORCA, is presented on the basis of multiple differential-drive robots. Formal proofs of collision-free motion (valid both for continuous and discrete control) are derived and several experiments are performed verifying the results. NH-ORCA achieves smooth and visually appealing trajectories for non-holonomic robots, as demonstrated in the first experiment. Furthermore,

the method successfully deals with very crowded situations, as shown in the second experiment with a larger group of fourteen robots.

In future work, it would be interesting to extend the method here presented to other non-holonomic vehicle dynamics. We believe this can be achieved by modifying the set of allowed holonomic velocities S_{AHV}. In accordance with [2], another line of research is to combine NH-ORCA with global path planning and to look closer at the avoidance of deadlock situations. For less controlled environments, or full integration of sensing and actuation, the method should be extended to compensate for uncertainties. Eventually, the method could be generalized for higher dimension and applied to underwater or aerial robots in $\mathbb{R}^3$.

References

1. Balkcom, D. J., Mason, M. T.: Time Optimal Trajectories for Bounded Velocity Differential Drive Vehicles. In: Int. J. Robot. Res. (21)(3), 199–218 (2002).
2. van den Berg, J., Guy, S. J., Lin, M. C., Manocha, D.: Reciprocal n-body Collision Avoidance. In: Proc. Int. Symp. Robot. Res., (2009).
3. van den Berg, J., Lin, M. C., Manocha, D.: Reciprocal Velocity Obstacles for real-time multi-agent navigation. In: Proc. IEEE Int. Conf. Robot. Autom., 1928–1935 (2008).
4. Borenstein, J., Koren, Y.: The vector field histogram - fast obstacle avoidance for mobile robots. In: IEEE Trans. Robot. Autom. (7), 278–288 (1991).
5. Chang, D. E., Shadden, S., Marsden, J. E., Olfati Saber, R.: Collision Avoidance for Multiple Agent Systems. In: Proc. IEEE Conf. Dec. Contr. (2003).
6. Fiorini, P., Shiller, Z.: Motion planning in dynamic environments using velocity obstacles. In: Int. J. Robot. Res. (17)(7), 760–772 (1998).
7. Guy, S. J., Chhugani, J., Kim, C., Satish N., Lin, M., Manocha, D., Dubey, P.: ClearPath: Highly Parallel Collision Avoidance for Multi-Agent Simulation. In: Proc. ACM SIGGRAPH Eurographics Symp. Comput. Animat. (2009).
8. Khatib, O.: Real-time obstacle avoidance for manipulators and mobile robots. In: Int. J. Robot. Res. (5), 90–98 (1986).
9. Lalish, E., Morgansen, K. A.: Decentralized Reactive Collision Avoidance for Multivehicle Systems. In: Proc. IEEE Conf. Decision and Control (2008).
10. Mondada, F., Bonani, M., Raemy, X., Pugh, J., Cianci, C., Klaptocz, A., Magnenat, S., Zufferey, J.-C., Floreano, D. and Martinoli, A.: The e-puck, a Robot Designed for Education in Engineering. In: Proc. Conf. Aut. Rob. Syst. Compet., 59–65 (2009).
11. Siméon, T., Leroy, S., Laumond, J.-P.: Path coordination for multiple mobile robots: a resolution complete algorithm. In: IEEE Trans. Robot. Autom. (18)(1) (2002).
12. Snape, J., van den Berg, J., Guy, S. J., Manocha, D.: Independent navigation of multiple mobile robots with hybrid reciprocal velocity obstacles. In: Proc. IEEE Int. Conf. Intell. Rob. Syst., 5917–5922 (2009).
13. Snape, J., van den Berg, J., Guy, S. J., Manocha, D.: S-ORCA: Guaranteeing Smooth and Collision-Free Multi-Robot Navigation Under Differential-Drive Constraints. In: Proc. IEEE Int. Conf. Robot. Autom. (2010).
14. Stipanović, D. M., Hokayem, P. F., Spong, M. W., Šiljak, D. D.: Cooperative Avoidance Control for Multiagent Systems. In: ASME J. Dyn. Sys. Meas. Control, (129)(5), 699–707 (2007).
15. Wilkie, D., van den Berg, J., Manocha, D.: Generalized velocity obstacles. In: Proc. IEEE Int. Conf. Intell. Rob. Syst., 5573–5578 (2009).